ELSEVIER

International Journal of Pharmaceutics 201 (2000) 221–237

international journal of pharmaceutics

www.elsevier.com/locate/ijpharm

Pharmaceutical relationships of three solid state forms of stavudine

R.B. Gandhi *, J.B. Bogardus, D.E. Bugay [1], R.K. Perrone, M.A. Kaplan [2]

Bristol–Myers Squibb Company, Pharmaceutics Research and Development, 1 Squibb Drive, NewBrunswick, NJ 08903, USA

Received 29 September 1999; received in revised form 30 March 2000; accepted 30 March 2000

Abstract

Three solid state forms of stavudine designated forms I, II and III have been identified and characterized. Forms I and II are anhydrous polymorphs whereas form III is hydrated and is pseudopolymorphic with forms I and II. Physico–chemical and thermodynamic properties of the three solid state forms have been characterized. Solid-state stability and potential for interconversion of the forms to aid in the selection of preferred form for development and commercialization has been studied. Conditions of recrystallization governing the formation of thermodynamically most stable polymorphic form I devoid of other forms was identified.

Keywords: Stavudine; Polymorphism; Dissolution; Hydrate; Nuclear magnetic resonance spectroscopy; Infra-red spectroscopy

1. Introduction

Stavudine (d4T: 2′3′-didehydro-3′-deoxythymidine) is chemically a thymidine nucleoside with inhibitory activity against reverse transcriptase of the human immunodeficiency virus (Hitchcock, 1991). The structure of stavudine is shown in Fig. 1. It has been shown to exist in three solid state forms designated as forms I, II and III. Forms I and II are anhydrous polymorphs, whereas Form III is hydrated [$(d4T)_3 \cdot H_20$]. The single crystal X-ray structure of forms I (Harte et al., 1991) and II (Gurskaya et al., 1991) has been reported previously. The present paper reports the physicochemical properties of three crystalline forms of stavudine. The different forms were characterized by determining thermal behavior, melting points, X-ray powder diffraction, infra-red spectroscopy, ^{13}C nuclear magnetic resonance spectroscopy, raman spectroscopy and solution calorimetry. Dissolution and solubility studies were also performed in aqueous and nonaqueous solvents to establish the thermodynamic relationships of the three forms. Variations are frequently found between batches or between sources of the same chemical sub-

* Corresponding author.

E-mail address: Rojesh.B.Gabdhi@bms.com (R.B. Gandhi)

[1] Present address: SSCI, Inc. 3065 Kent Avenue, West Lafayette, IN 47906, USA.

[2] Present address: 1026, Glencove Road, Syracuse, NY 13206, USA.

0378-5173/00/$ - see front matter
PII: S0378-5173(00)00419-1

stance. In seeking explanations for such variations, experimenters have traditionally used chemical analyses for impurities or hydration level (Hendriksen, 1989). Awareness of possible habit or polymorphic differences has led to the examination of this phenomenon more frequently and closely (Haleblian and McCrone, 1996). In the present work, variations between batches of stavudine have been systematically examined. In some cases, the variations were unplanned (samples from production line). Another objective of the present work was to conduct recrystallization studies to define conditions which could reproducibly yield pure form I, since this form was preferred for development because it is thermodynamically more stable than forms II and III.

2. Materials and methods

2.1. Materials

Stavudine was manufactured by Technical Operations Division of Bristol–Myers Squibb, Syracuse, NY. All water used was double distilled and deionized. All other reagents were analytical grades unless otherwise stated.

2.2. Powder X-ray diffraction

X-ray powder diffraction patterns of the three forms were recorded using a Rigaku Geigerflex diffractometer with a vertical goniometer in the $\theta/2\theta$ geometry. The X-ray generator was operated at 45 kV and 40 mA with a copper radiation source. X-ray powder diffraction was also performed on stability samples to study solid state transformations on excess solid remaining at the conclusion of the dissolution. Samples were scanned between 5° and 40° 2θ at a speed of 2° 2θ/min.

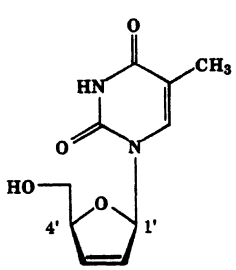

Fig. 1. Structure of D4T.

2.3. Optical microscopy studies

The morphologies of samples of three polymorphic forms were evaluated for crystal size and shape using an Olympus BHA polarizing microscope. The samples were mulled in mineral oil on a glass slide and immobilized with a coverslip. Owing to the fine particle size of the material, all observations were made at 80–200 × magnifications. Polarizing optics were used to study the crystallographic properties of the solids.

2.4. Differential scanning calorimetry

Differential scanning calorimetry thermograms were acquired using a TA Instruments DSC 2910 with Thermal Solutions data analysis software. The sample was placed in an aluminum pan in which a pinhole was punched in the pan lid. Samples were scanned at a rate of 10°C/min from 50–250°C. The instrument was calibrated with indium (mp 156.6°C, heat of fusion 28.4 J/g).

2.5. Thermogravimetric analysis and hot stage microscopy

Thermogravimetric analysis (TGA) was performed on each form using a Perkin Elmer TGS-2 Balance control with Thermal analysis data station to study the amount and temperature range of loss of volatiles. TGA was performed with each sample at a heating rate of 2°C/min, from 30 to 230°C, in nitrogen atmosphere.

In order to confirm the thermal events observed by TGA, hot stage microscopy studies were performed on a Mettler FP 82 hot stage using McCrone Thermal analysis software. A sample of the solid was suspended in silicone oil and monitored under a polarized light microscope. The three forms were heated in silicone oil from 30 to 170°C at 5°C/min.

2.6. Variable temperature X-ray diffraction

Powder X-ray diffraction (XRD) measurements were obtained on Philips XPERT system, using copper radiation with generator settings of 45 kV and 40 mA. Each sample was scanned between 2 and 32 deg 2θ and in step sizes of 0.03 deg 2θ. Philips APDW software was used for all data collection and data analysis.

2.7. Fourier transform infra-red (IR) spectroscopy

IR spectra were obtained on a Nicolet model 740 spectrophotometer in the mid and near-IR regions. For mid-IR spectra, the spectrophotometer was configured with a water-cooled globar source, Ge/KBr beamsplitter and a liquid nitrogen cooled mercury cadmium telluride (MCT-A) detector. Near-IR spectra were acquired with a quartz beamsplitter and a PbSe detector. All spectra represent 64 co-added scans acquired at a spectral resolution of 4 cm^{-1}. Dry air or nitrogen was used to purge the optical bench during spectral acquisition. A Spectra-Tech Collector™ diffuse reflectance sampling accessory was used for analysis. Approximately 500 mg of sample was placed into the 13 mm diameter macro sampling cup and a single beam data file generated. An identical cup filled with KBr was used for acquisition of the background data file. Subsequently, the two data files were ratioed to obtain a frequency domain spectrum represented in log 1/reflectance units. The variable temperature IR spectra were collected with the same diffuse reflectance sampling accessory adapted with a controlled environmental chamber. The temperature of the chamber was controlled by an Omega CN-2010 series programmable temperature controller. A Welch vacuum pump was used to obtain a 5 ± 1 mmHg vacuum in the chamber.

2.8. Raman spectroscopy

Raman spectra were acquired on a Nicolet model 910 Fourier transform (FT) Raman spectrometer operating with a Nd:YAG laser (1064 nm) set at a power of approximately 700 mW. The spectra were acquired using 180° collection reflective optics. Sample preparation involved packing a 5 mm NMR tube with approximately 50 mg of material and placing the tube in the spectrometer.

2.9. ^{13}C Nuclear magnetic resonance spectroscopy

The solid-state ^{13}C NMR spectra were obtained on a Bruker AM-250 spectrometer utilizing a ^{13}C resonant frequency of 62.9 MHz (magnetic field strength of 5.87 T). Approximately 500 mg of sample was lightly packed into a zirconium rotor with a Kel-F cap. The cross polarization, magic angle spinning (CP/MAS) pulse sequence was used for spectral acquisition. Each sample was spun at a frequency of 5.0 ± 0.01 kHz and the magic angle setting calibrated by the KBr method (Frye and Maciel, 1982). Each spectrum represents between 5 and 9k transients acquired under the following conditions: 4k data set zero filled to 16k, spectral width of 20 000 Hz, 5 s recycle time, 2 ms contact time, and 7.4 μs pulse width. The Hartmann–Hahn match was optimized by monitoring the ^{13}C intensity versus ^{13}C radio frequency field with a spinning adamantine sample. Each data set was subjected to a 5.0 Hz line broadening factor and subsequently Fourier transformed and phase corrected to produce a frequency domain spectrum. All spectra were recorded at ambient temperature and the chemical shifts externally referenced to tetramethylsilane utilizing a spinning adamantine sample $[\delta(CH_3)_4Si = \delta(\text{adamantine } CH_2) - 38.3]$.

2.10. Moisture sorption/desorption studies

The initial water contents of all three forms were determined by Karl Fischer titration. The rate and extent of moisture sorption under different humidity conditions were determined using a Cahn Digital Recording Balance fitted with a system to maintain and monitor specific relative humidity conditions. Various salt solutions (LiCl, NaCl, $MgCl_2$, K_2SO_4) at room temperature were used to maintain different relative humidity conditions.

2.11. Dissolution in aqueous and non-aqueous solvents

Weighed samples of the three forms of stavudine, approximately two to three times the amount necessary to saturate the solution, were placed in 20 cc glass vials containing the appropriate solvent (water or isopropanol). The solvent was previously equilibrated at 25°C. The solution was stirred at 90 rpm using a magnetic stirrer. The vials were stoppered and placed in a jacketed beaker maintained at 25°C. Periodically samples were withdrawn from the vials, filtered through Acrodisc® filters and diluted appropriately with dissolution media. The stavudine concentrations were measured spectrophotometrically at 265 nm.

2.12. Solution calorimetry

The heat of solution of three forms of stavudine was measured at 25°C in water using Thermometric 2225 precision solution calorimeter and its accompanying software SolCal®. Samples of approximately 30 mg were weighed into a 1 ml glass ampule and sealed with a glass stopper using melted wax. The sample ampoules are sufficiently thin so that no measurable heat effect is produced due to breaking of the glass. The heats of solution were measured by breaking the sample bulbs in the reaction vessel containing 100 ml of solvent. The system was calibrated electrically by passing a measured current through a calibration heater for a measured length of time such that the calibration energy was approximately equal to the heat absorbed in the heat of solution measurement. The time versus the temperature history of the calibration and reaction period was monitored. The accuracy of the method was checked by measuring the heat of solution of TRIS in 0.1 M HCl. The value agreed in all cases within 2% of the accepted literature value of 29.7 kJ/mol at 25°C (Hill, et al., 1969).

2.13. Conversion to thermodynamically stable pure form I from mixtures of polymorphs

Since polymorphic form I is the most stable form at room temperature several approaches were evaluated to obtain pure polymorphic form I devoid of forms II and III during the final recrystallization step. In the first approach the samples were heated in an oven at 70–80°C for 24 h. Alternatively, some lots were recrystallized from isopropanol. A suspension of stavudine at 70°C was filtered and the filtrate was seeded with form I and cooled with a controlled temperature drop to room temperature. The solid was then filtered and analyzed by powder X-ray diffraction.

3. Results and discussion

3.1. Physical and chemical characterization

Characterization of several lots of stavudine bulk drug substance indicated the existence of three distinct crystalline forms designated as forms I, II and III. Form I appeared as rectangular large rods, form II as short needles or rods, and form III as irregular shards.

Forms I, II, and III can be distinguished by their characteristic powder X-ray diffraction pattern which are shown in Fig. 2a–c, respectively. The unique characteristic scattering angles 2θ that can distinguish any form from the mixture is 19.1° for form I, 11.2° and 18.6° for form II; and 15.5° for form III as shown in Fig. 2.

DSC data of the three polymorphic forms is presented in Fig. 3. Forms I and II exhibit melting onset at 171.6 and 168.9°C, respectively. Form III exhibits a broad exotherm at 141.9°C and an endotherm at 171.3°C. Melting of all three forms was consistently followed by an endotherm representing decomposition.

Hot stage microscopy showed the melting of forms I and II in the range of 168–172°C. The melting of the crystal was followed by the appearance of the crystals of the decomposition product of stavudine (thymine). No apparent changes occurred in the crystal structure of forms I and II upon heating. In contrast, form III showed vigorous bubble formation when heated in silicone oil around 118°C, suggesting the possibility of a hydrate. The bubble formations at a temperature higher than 100°C suggests that this water is bound strongly to the crystal lattice and is not

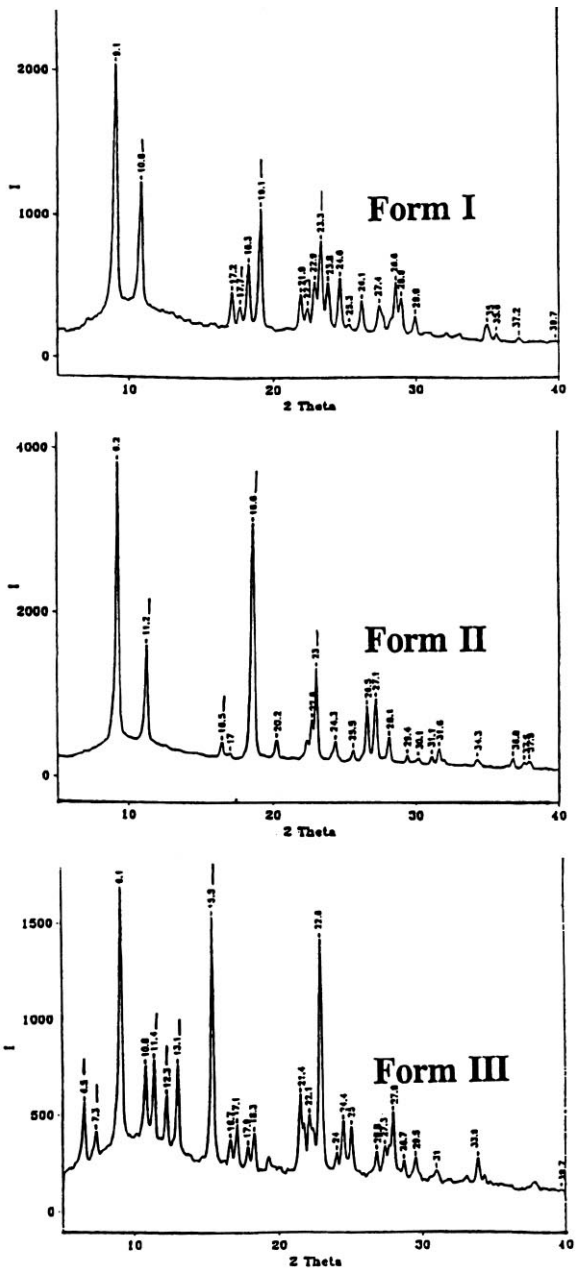

Fig. 2. X-ray power diffraction of three forms of D4T.

'surface water'. This thermal technique could distinguish form III from forms I and II. Also as shown in Fig. 4, the material exhibited a solid state transformation between 121 and 153°C. Subsequent to melting of stavudine, thymine crystallized from the melt (frames e and f). In order to gain an understanding of the exotherm at 141.9°C for form III, further experiments were conducted using variable temperature powder X-ray diffraction (VT-XRD). The pattern of VT-XRD (Fig. 5) confirms the conversion of form III to form I as shown by the exothermic solid state transformation whose maximum is at 141.9°C in the DSC curve of neat form III material and by hot stage microscopy. The powder XRD pattern of the initial form III heated at 155°C and cooled to 25°C is similar to form I with a small trace of form II.

The three forms of stavudine were examined by mid and near-IR spectroscopy. In the mid-IR spectral region, very similar spectra were measured for each crystal form. Form I display distinct reflectance bands at 3528, 3425, and 865 cm^{-1}, whereas form II has unique bands at 3485 and 975 cm^{-1}, and form III has a unique peak at 3510 cm^{-1}. Although these unique reflectance bands are noted, these minor spectral differences do not allow for the unequivocal physical identification of samples or mixtures by mid-IR. It is important to note that the mid and near-IR spectra were acquired utilizing the diffuse reflectance technique in which the sample is simply placed into a cup holder and examined by the spectrophotometer. Acquisition of the mid-IR spectra by the alkali halide (KBr) pellet sample preparation technique produced spectra slightly different from the diffuse reflectance spectra. Some absorption bands in the KBr spectra were shifted by at least 5–10 cm^{-1} as compared to the diffuse reflectance spectra. These spectral shifts can be attributed to perturbations upon the structure (environment) of various chemical moieties caused by the extreme pressure and slight temperature conditions imposed by the sample preparation conditions of the alkali halide pellet sample preparation technique. Therefore, it is recommended that when one utilizes IR spectroscopy for the physical characterization of materials, the diffuse reflectance sampling technique is employed.

Near-IR proved to be a valuable technique for the characterization of the different crystal forms of stavudine. Upon comparison of the three near-

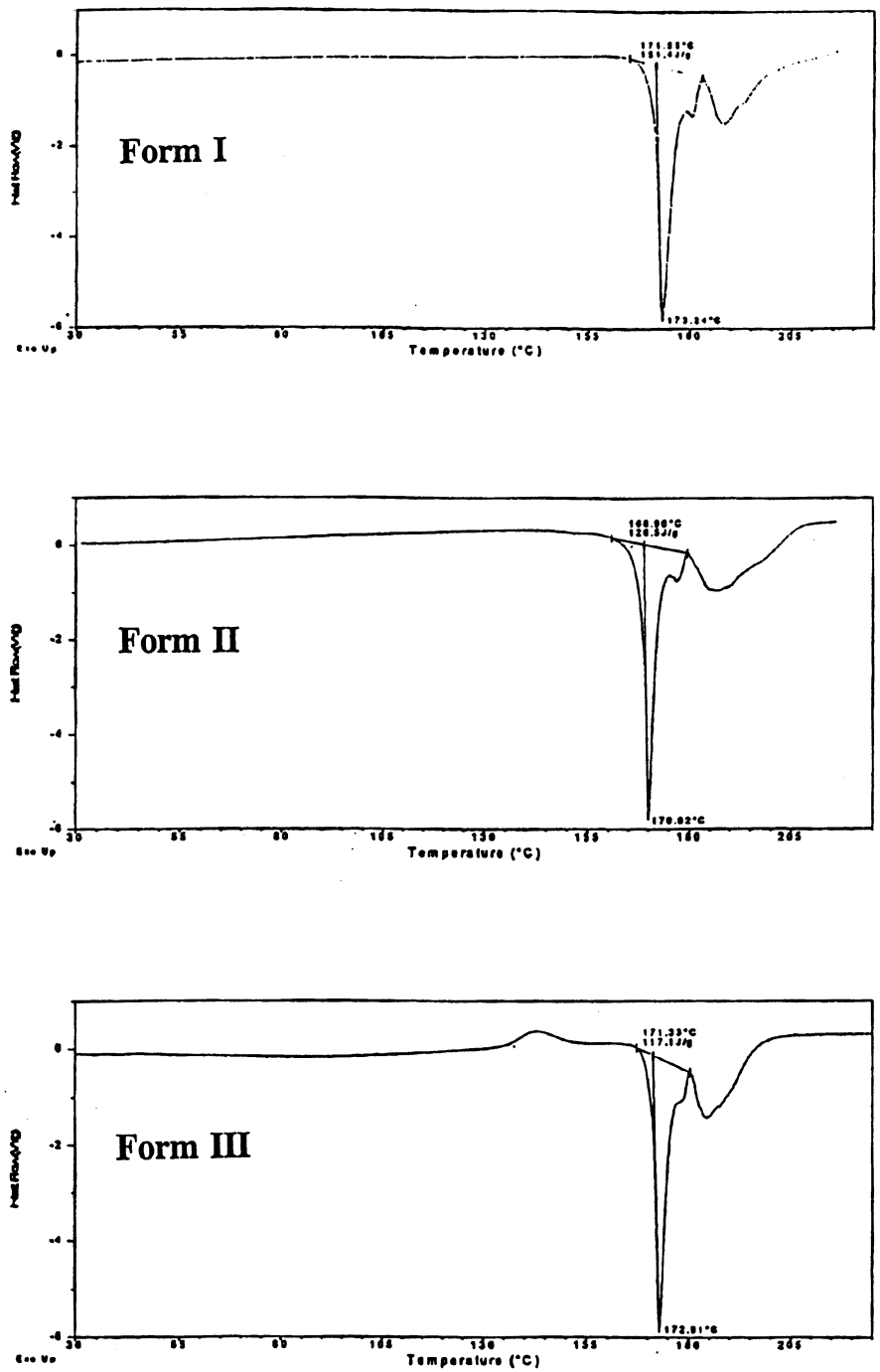

Fig. 3. Differential scanning calorimetry of three forms of D4T.

IR spectra (Fig. 6), it is clearly evident that form III material has a distinct reflectance band at 5137 cm^{-1} as well as each crystal form displaying some unique spectral features. Based upon thermal analysis and KF moisture data, it was postulated that form III was a hydrate. Near-IR data was used to confirm this hypothesis. The hydrate –OH moiety is known to have a combination band (~ 5100 cm^{-1}) in the near-IR spectral region (Osborn and Fearn, 1986). Additionally, variable

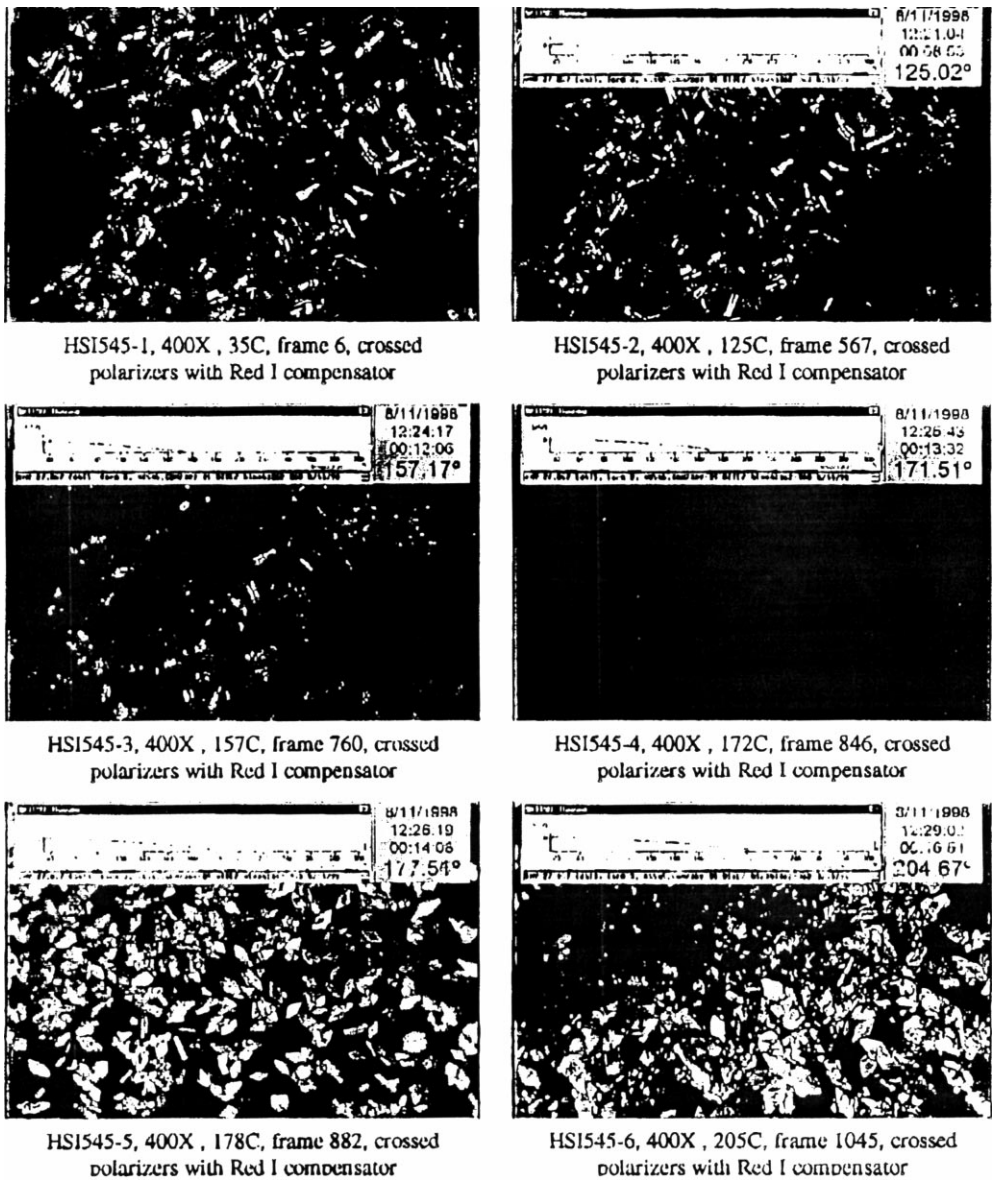

HSI545-1, 400X , 35C, frame 6, crossed polarizers with Red I compensator

HSI545-2, 400X , 125C, frame 567, crossed polarizers with Red I compensator

HSI545-3, 400X , 157C, frame 760, crossed polarizers with Red I compensator

HSI545-4, 400X , 172C, frame 846, crossed polarizers with Red I compensator

HSI545-5, 400X , 178C, frame 882, crossed polarizers with Red I compensator

HSI545-6, 400X , 205C, frame 1045, crossed polarizers with Red I compensator

Fig. 4. Hot stage digital video microscopy of form III. (a) Initial, (b) 125.0, (c) 157.2, (d) 171.5, (e) 177.5 and (f) 204.7°C.

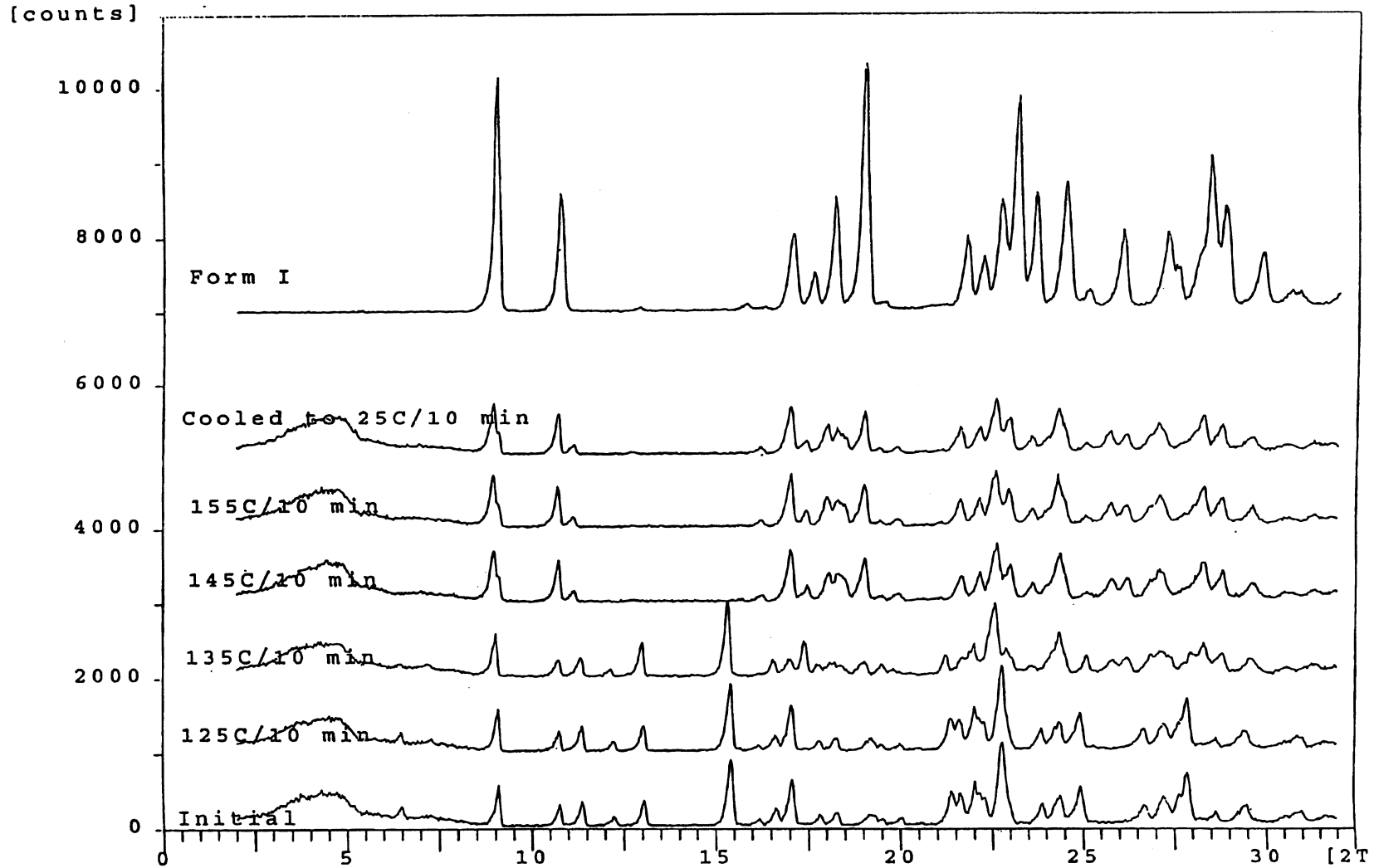

Fig. 5. Variable temperature X-ray diffraction of form III.

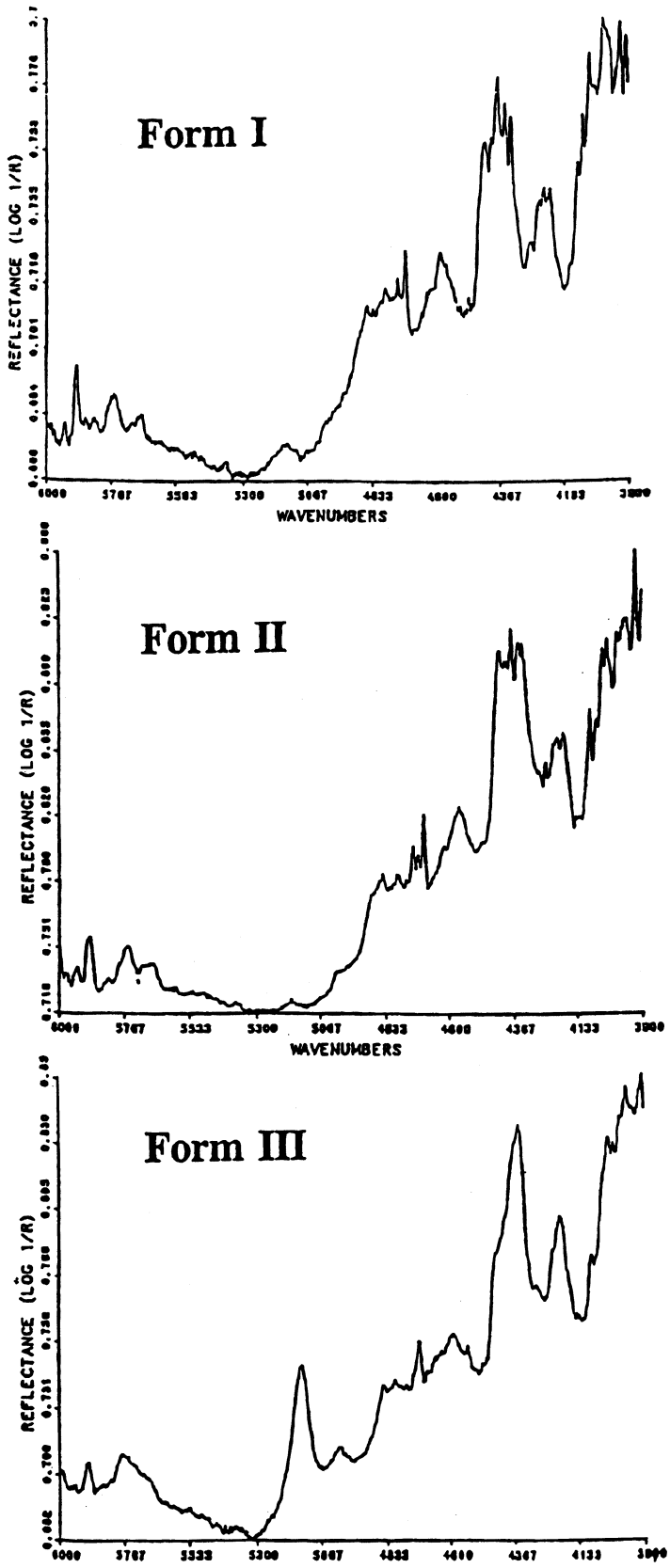

Fig. 6. FTIR spectra of three forms of D4T in mid-IR region.

temperature near-IR diffuse reflectance spectroscopy was used to further confirm the hydrate character of form III. Form III material was maintained at 80°C for 1 h and spectra collected every minute. The spectral feature at 5137 cm^{-1} decreases in intensity over time. The facts that this peak correlates to the combination –OH vibrational mode, water content analysis by Karl Fischer titration indicates a 3:1 ratio of drug:water, and the 80°C IR experiment shows that only this spectral feature changes upon heating, unequivocally confirm the hydrate character of form III. It is interesting to note during the 80°C IR experiment, only the 5137 cm^{-1} peak diminished in intensity over time, but the –OH dihydrofurfuryl alcohol moiety (3360 cm^{-1}) shifted to higher frequency (3425 cm^{-1}) upon dehydration. The increase in vibrational frequency can be attributed to the greater degree of flexibility of the alcohol moiety as the hydrogen bonding decreases during dehydration. This seems to indicate that the site of hydrogen bonding of the hydrate to the stavudine molecule is at the dihydrofurfuryl alcohol. Other sites of hydrogen bonding are the carbonyls of the thymine ring. Since no shift in the carbonyl vibrational frequencies were noted during the dehydration experiment, it appears as if the hydrate hydrogen bonding occurs with the dihydrofurfuryl alcohol moiety.

FT-Raman spectra were also acquired on the three forms of stavudine. Virtually no spectral differences are noted for the three spectra except in the C–H stretching region ($3150 - 3000\ cm^{-1}$). Although some minor spectral differences exist between the three forms of stavudine, the small magnitude of the differences and slight difficulty in obtaining good signal-to-noise spectra, prevent quantitative analysis by FT-Raman spectroscopy.

The qualitative solid-state ^{13}C NMR spectra of the three forms of stavudine are presented in Fig. 7. Distinct spectra are measured for each form indicating the unique chemical environment of the carbon nuclei in each crystal form. Spectral assignments for the solid-state spectra are presented in Table 1 and are based on the original solution-phase NMR assignments. The two carbonyl and thymine C2′ resonances for all three crystal forms are fairly broad due to dipolar coupling to the adjacent nitrogen atoms. Additional dipolar coupling is displayed in the C1 resonance for form I ($d = 90.0$, 88.4 ppm), form II ($d = 94.5$, 92.9 ppm), and form III ($d = 87.8$, 86.7 ppm). Splitting due to the dipolar coupling aids in the spectral assignments.

For forms I and II, it appears that the thymine ring is locked into an equivalent conformation. Less than a 0.5 ppm chemical difference exists between respective carbons (C2′, C3′, C4′, and C6′) in each form. The thymine ring for form III appears to be in a slightly different conformation. The most notable chemical shift difference being for carbon C6′. The carbonyl resonance displays two resonances for form III probably due to dipolar coupling to the adjacent nitrogen atom. The remaining thymine resonances (C2′, C3′, and C4′) display chemical shift differences as compared to their respective carbons in forms I and II, thus supporting the claim of a slightly different confirmation of the thymine for form III. Nonequivalent chemical shift values for carbons C1, C2, C3, and C4 in each crystal form indicate that the dihydrofurfuryl alcohol ring is in distinctly different conformations. It is interesting to note that although the dihydrofurfuryl alcohol ring has a slight change in conformation for each crystal form, the alcohol carbon resonance (C5) is virtually unchanged for each form ($d = 62.6$ ppm). Based upon the IR data, this chemical moiety appears to be involved in hydrogen bonding of the form III hydrate structure.

One of the most significant differences in the solid-state ^{13}C NMR spectra for each crystal form originates from the single methyl group attached to the thymine ring. For form I, a single resonance ($d = 14.0$ ppm) is observed. The methyl resonance for forms II and III display a doublet, yet the doublet exists at different chemical shift values for each crystal form (Table 1). The doublet resonance of the methyl group in forms II and III may be attributed to either: (1) long range dipolar coupling to the nitrogen atoms, or (2) crystallographically nonequivalent sites in the unit cell for the methyl group. Since the nitrogen atoms are three bonds removed and the magnitude of dipolar coupling is related to $1/r^3$ (r = distance between atoms), it is relatively unlikely that

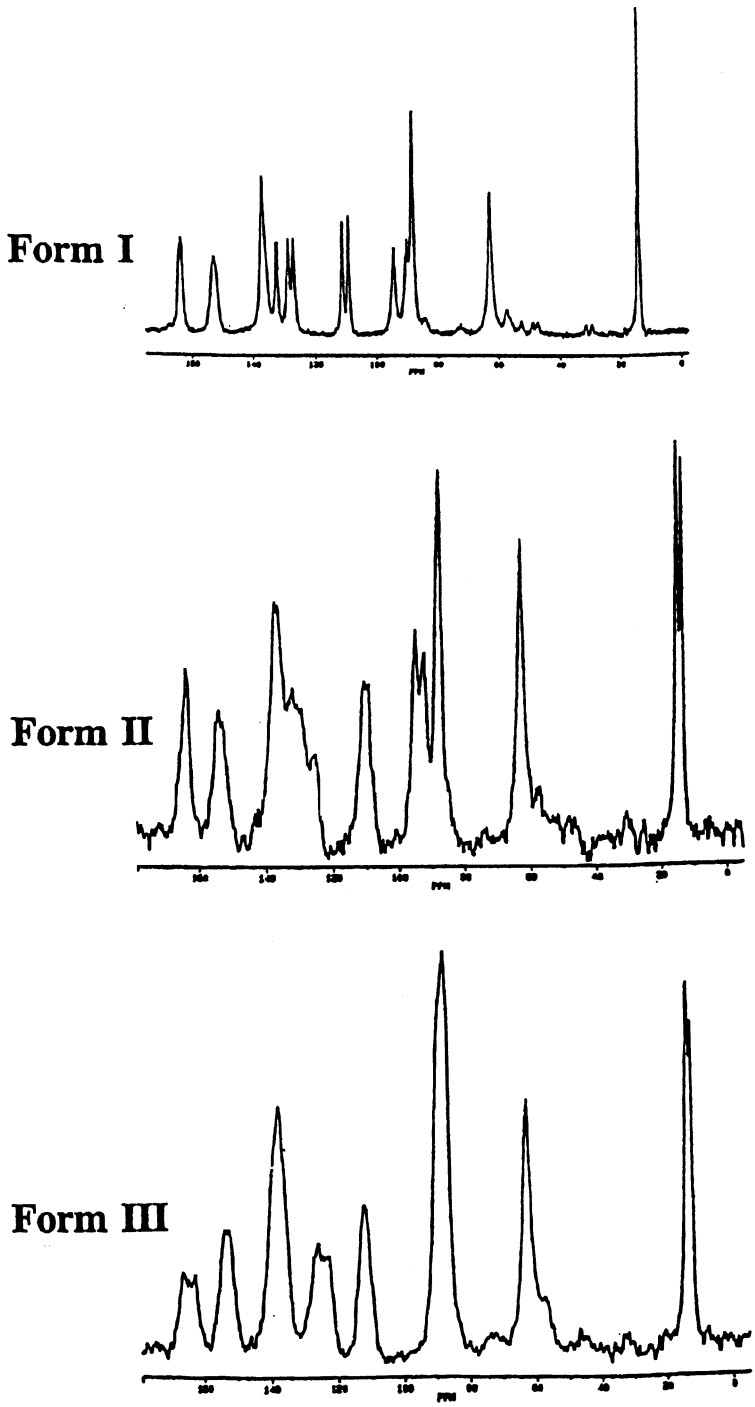

Fig. 7. ^{13}C NMR spectra of three forms of D4T.

the methyl doublets are due to dipolar coupling. Instead, the doublet resonances of the methyl group in forms II and III are due to 'crystallo graphic splitting'. This phenomenon arises from the fact that more than one methyl group is contained within the unit cell and the carbon atom for each of these two methyl groups is in a slightly different chemical (magnetic) environment. From a quantitative perspective, the distinct differences in the solid-state ^{13}C NMR spectra for each form of stavudine permits quantitative assessment of phase purity for batches of drug substance.The initial moisture content as determined by Karl Fischer titration of form I and II were less than 0.5% but form III showed moisture content of 2.4%, corresponding to 0.32 mol of water per mole of stavudine. TGA experiments showed no weight loss of forms I and II up to 160°C. Form III showed approximately 2.1% weight loss from 60 to 120°C. On a molar basis this corresponds to 0.28 mol of water per mole of stavudine, or an approximate stavudine:water stoichiometry of 3:1. These results are consistent with the initial moisture content determined by Karl Fischer titration.

Table 1
Solid-state ^{13}C NMR peak assignments

Carbon designation[a]	Chemical shift (ppm)[b]		
	Form I	Form II	Form III
C4′ = O	164.0	164.0	166–163
C6′ = O	152.9	153.0	152.6
C2′	137.0	137.6	139–136
C2	132–127	132–125	126–122
C3	132–127	132–125	126–122
C3′	111, 109	111, 109	112, 110
C1	94–88	94–87	88–86
C4	94–88	94–87	88–86
C5	62.7	62.3	62.6
C3′CH_3	14.0	15.0, 13.5	13.8, 12.6

[a] Numbering scheme based on Fig. 1.
[b] All chemical shifts externally referenced to TMS.

Table 2
Transformation studies of D4T under stress conditions

Conditions	Form I	Form II	Form III
50°C/4 weeks	I	II	III
60°C/24 h per vacuum	I	II	III
80°C/24 h per vacuum	I	II	I

The moisture uptake of the three forms was determined by Cahn moisture balance studies. Forms I and III are non-hygroscopic while form II shows slight increase in weight (0.4% w/w) at very high humidity (> 90% RH). Samples exposed at high humidities showed no evidence of degradation to thymine when analyzed by HPLC indicating good chemical stability. A hydrate may lose water at low humidities. However, form III showed no significant change in moisture content after 10 weeks at 25°C/21% RH. This suggests that the water is tightly bound to the crystal lattice via strong interactions confirming the results of TGA.

The effect of temperature stress on interconversion among the three solid state forms of stavudine was studied as shown in Table 2, none of the three forms show interconversion at 50°C through 4 weeks. At 60°C/24 h under the vacuum, form III lost most of its moisture but the X-ray pattern did not show any transformation. At 80°C/24 h under vacuum, form III lost most of its water and transformed to form I as shown by X-ray powder diffraction pattern. Forms I and II showed no conversion under these conditions. These results suggest that under the experimental conditions tested, form I and II do not undergo polymorphic transformation. Form III can be converted to form I when heated for 24 h under the vacuum at 80°C or higher. This conversion was also evident by FTIR spectroscopy in the mid IR region.

3.2. Dissolution of three forms in aqueous and non-aqueous solvents

The solubility and dissolution profiles of the three forms in water at 25°C are shown in Fig. 8. These plots show the concentration achieved in solution for each form as a function of time, in the presence of an excess solid phase and under essentially constant agitation. It is apparent from the data that form II has a higher instantaneous

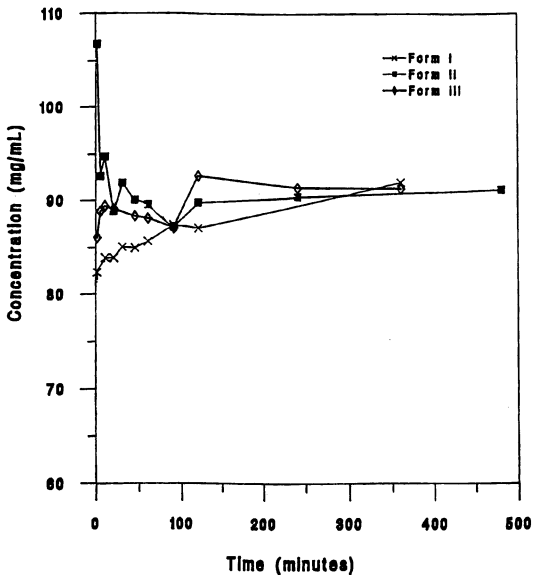

Fig. 8. Dissolution of three forms of D4T in water at 25°C.

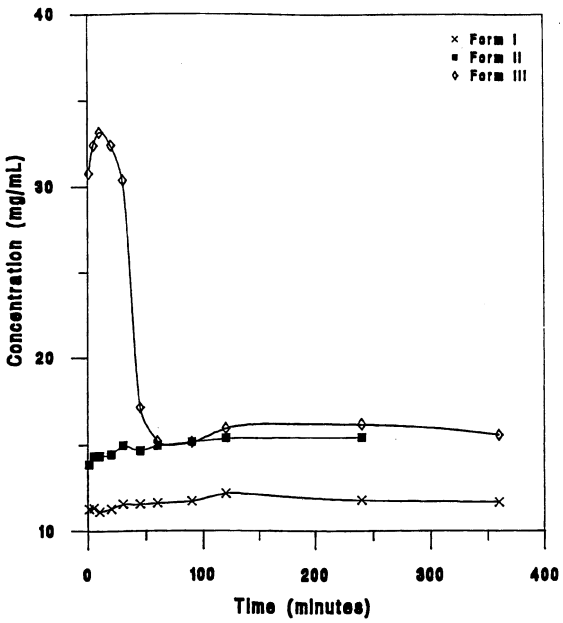

Fig. 9. Dissolution of three forms of D4T in isopropanol at 25°C.

concentration (106.8 mg/ml) than the other two forms. The instantaneous maximum concentration is an estimate of apparent solubility, since the sampling at initial time period was performed as frequently as experimentally possible. After form II reaches the maximum concentration, there is a decline in the amount of the drug dissolved. The mean limiting value of this decrease was found to be the solubility of form III (90.6 mg/ml). The solvent mediated conversion to form III at the end of experiment was confirmed by X-ray diffraction analysis. Form I showed the lowest mean apparent solubility (88.8 mg/ml) among the three forms without any solvent mediated conversion upto 6 h in water.

Frequently in aqueous systems an anhydrate is more soluble than a corresponding hydrate. In organic solvents, however, the hydrate is expected to be more soluble than the anhydrate (Shefter and Higuchi, 1963). To investigate this behavior with stavudine, dissolution studies were performed in isopropanol. (Fig. 9). In isopropanol, form III has a higher dissolution rate and apparent saturation concentration than the other two forms. After about 4 h, however, the apparent solubility of form III decreased from 33.1 to 15.6 mg/ml. X-ray diffraction analysis of solid isolated at the end of the experiment revealed the transformation of form III to form II. X-ray diffraction analysis of the solid at the end of dissolution experiment with forms I and II did not show any change in the crystal forms. The reversion in solubilities of form II and form III in aqueous and organic solvent, respectively, supports the conclusion that form III is a true hydrate (not surface bound water). As in water, solubility of form I was the lowest (11.6 mg/ml) among the three forms in isopropanol. The solubility of form I is lowest in both aqueous and organic phases and form I does not undergo solvent-mediated conversion under experimental conditions. These findings confirm that form I is more thermodynamically stable than forms II and III.

3.3. Thermodynamics

The solubilities of the three forms in water as described in the dissolution experiments suggest that the energy difference among the three forms is small. X-ray diffraction studies show that suspensions of form II can convert to form III in water.

The changes in the heat content for the hydration of form II in water can be calculated from the enthalpy changes of the following reaction.

$$A_{solid} \Leftrightarrow A_{aqueous} \quad \text{(Form II)} \tag{1}$$

$$A{:}XH_2O_{solid} \Leftrightarrow A_{aqueous} + XH_2O_{liquid} \quad \text{(Form III)} \tag{2}$$

Subtracting Eq. (2) from (1) gives

$$A_{solid} + XH_2O_{liquid} \Leftrightarrow A{:}XH_2O_{solid} \quad \text{(Form II) (Form III)} \tag{3}$$

The heat of solutions of forms II and III are the heat of reactions of Eq. (2) and (3). Hence the enthalpy of hydration can be calculated from the heats of solutions in water. The heats of solutions of three forms were determined using a solution calorimeter. Table 3 shows the heat of solutions of three forms in water at 25°C. The standard deviations on the measurements of heat of solutions of the three forms were within 0.2 kJ/mol. From the dissolution data in water, using the maximum concentration as an estimate of its solubility, the free energy of hydration can be calculated (Shefter and Higuchi, 1963). At constant temperature and pressure, the free energy difference between the anhydrous and hydrated forms is determined by the following equation:

$$\Delta F_T = \frac{RT \quad \ln\ (C_s)\ \text{anhydrous}}{(C_s)\ \text{hydrate}} \tag{4}$$

This equation relates the solubility C_s, of forms II and III at a particular temperature T, to the free energy difference. This ΔF_T corresponds to the free energy of hydration since the activity of water is approximately unity in the present system. The free energy change for hydration of form II to III so calculated is 407.3 J/mol. Using Eq. (4), the free energy of hydration of form I to III was determined to be 457.1 J/mol. The enthalpy of hydration of forms I and II are 1.5 and 0.8 kJ/mol, respectively. The entropy change during hydration reaction ΔS_T can be calculated at a particular temperature using the following equation:

$$S_T = (\Delta H_T - \Delta F_T)/T \tag{5}$$

The entropy change for hydration so calculated for form I and II is a small positive number, i.e. $+0.84$ and $+0.32$ e.u., respectively. The entropy change involved in fusion of water is approximately -6 e.u. (Sutor, 1958). Form III is a hydrate and three molecules of stavudine combines with a single molecule of water. Therefore, one does not expect water molecules to form a chain network throughout the lattice. This type of structure could be responsible for the small increase in entropy associated with the transformation of the dehydrated form to the hydrated form.

Enantiotropic polymorphs can be interconverted below the melting point of either polymorph, while monotropic polymorphs cannot (Burger and Ramberger, 1979). Thermal characteristics such as melting points of forms I and II are similar. The heat of fusion can be determined only approximately since the melting of each form is followed immediately by decomposition. Therefore, heat of fusion rule could not be used to determine whether forms I and II are related enantiotropically or monotropically. Fig. 10 shows a plot of ln solubility versus $1/T$ for forms I and II in isopropanol over the temperature range of 50–70°C. The van't Hoff plot is non-linear and it is apparent from the plot that solubility of form II is greater than form I in this tempera-

Table 3
Thermodynamic parameters calculated for the three polymorphic forms of D4T

Form	Heat of solution (kJ/mol)	Enthalpy change ΔH (kJ/mol)	Free energy change ΔG (J/mol)	ΔS_{298} (e.u.)
I	13.8	$1.5_{I \rightarrow III}$	$457.1_{I \rightarrow III}$	0.84
II	13.1	$0.8_{I \rightarrow III}$	$407.3_{I \rightarrow III}$	0.32
III	12.3	—	—	—

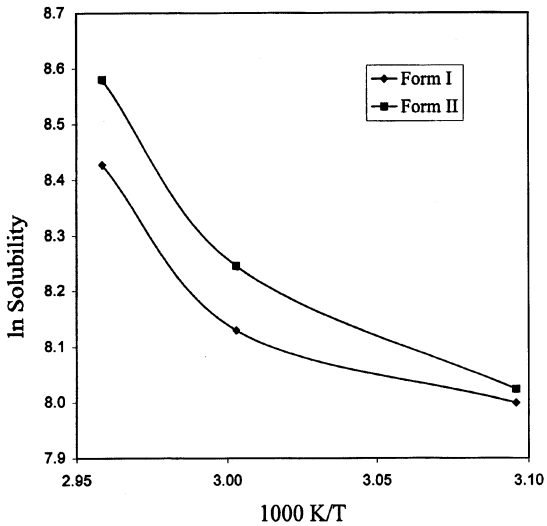

Fig. 10. Plot of ln S versus $1/T$ for D4T.

Table 4
Effect of short-term exposure to heat on polymorphic composition of D4T

Lot no.	Conditions (°C/h)	Initial peaks	Final peaks
1	70/24	I & II[a]	I[b]
	80/18	I & II[a]	I[b]
2	70/3	I & II[a]	I & II[a]
	70/24	I & II[a]	I, II[a,b]
3	70/6	I & II	I, II[b]
	70/24	I & II	I, II[b]
	80/18	I & II	I, II[b]

[a] Predominantly form I with shoulder peaks of form II.
[b] Also contains minor unidentified peaks.

ture range. The solubility difference decreases as the temperature decreases. Therefore, it appears that forms I and II are related enantiotropically. Because limited data points covering a relatively narrow range of temperature were available, the data could not be treated by multiple regression analysis using the equation recommended by (Grant et al., 1984) for the curve fitting. Therefore, the heat of solutions for each form was calculated only calorimetrically.

3.4. Conversion of mixtures of polymorphic forms to pure form I

The stavudine obtained is usually recrystallized from hot organic solvent solution as the final step in the process. During the course of process development and scale-up, several recrystallization schemes were investigated. Initially, the pilot plant recrystallization process involved cooling of hot isopropanol solution from 75–82 to 65–75°C over 1 h and then to 0–5°C over 1.5 h. This procedure yielded form II, or mixtures of form I and II, which was not desirable. Several lots of stavudine were manufactured and recrystallized from isopropanol. These lots were found to be a mixture of forms I and II in significant proportion as shown by X-ray powder diffraction patterns. Form I has been found to be more thermodynamically stable, with no tendency for solid state conversion. Experiments were conducted to reliably, conveniently and reproducibly prepare stavudine form I.

The effect of short-term exposure to heat on several bulk lots with a mixture of two forms were attempted to obtain pure form, as shown in Table 4, short-term heat treatment did not reproducibly yield pure form I from a mixture of forms I and II. Hence crystallization conditions were closely monitored to yield pure form I. Crystal growth processes are determined by mass transfer (diffusion) and by the kinetics and attachment of molecules to crystals. These processes determine not only the growth rate and shape of the crystals but also its composition and degree of perfection. To aid in process development, some of the parameters such as the rate of cooling or stirring, which might affect recrystallization from isopropanol, were studied. Table 5 shows the effect of stirring and the rate of cooling on four lots of stavudine during recrystallization from solution in isopropanol. This solution was obtained after filtration of a slurry of stavudine in isopropanol at 70°C as described in the experimental section. Powder X-ray diffraction analyses on the initial Lots 1–4 samples and the final solid products obtained after the recrystallization were used to identify the presence or absence of form I and II. As shown in Table 3, all lots during recrystalliza-

Table 5
Effect of stirring and rate of cooling on various lots of D4T during recrystallization from isopropanol

Lot no.	Conditions	Initial D4T product	Final D4T product
1 (a)	w/stirring; 10°C/30 min	I & II[a]	I[b]
1 (b)	w/stirring; 5°C/30 min	I & II[a]	I
1 (c)	w/o stirring; 5°C/30 min	I & II[a]	I & II
1 (d)	w/stirring; 10°C/15 min (held for 1 h after each 10°C drop)	I & II[a]	I
2 (a)	w/stirring; 10°C/30 min	I & II[a]	I
2 (b)	w/stirring; 5°C/30 min	I & II [a]	I
2 (c)	w/o stirring; 5°C/30 min	I & II [a]	I & II
2 (d)	w/stirring; 10°C/15 min (held for 1 h after each 10°C drop)	I & II[a]	I
3 (a)	w/stirring; 5°C/30 min	I & II	I[b]
3 (b)	w/o stirring; 5°C/30 min	I & II	I, II[b]
3 (c)	w/o stirring; very rapid cooling	I & II	II[b]
3 (d)	w/stirring; 10°C/15 min (held for 1 h after each 10°C drop)	I & II	I
4	w/o stirring; very rapid cooling	I & II[a]	I, II[b]

[a] Predominantly form I with shoulder peaks of form II.
[b] Also contains minor unidentified peaks.

tion, if left unstirred resulted in a mixture of I and II. However, when the solution was stirred with slow cooling, pure form I could be obtained. For example, a solution of 3(c) when cooled very rapidly, gave mostly form II. When a solution of Lot 2(a) is slowly cooled at the rate of 10°C/30 min form I is obtained. When a solution of Lot 1(a) was cooled at the rate of 10°C/30 min the X-ray pattern indicated the presence of form I and some other unidentified component. Cooling at a slower rate (5°C/30 min) or cooling at 10°C/15 min with 1 h hold at the temperature after each drop, gave the X-ray pattern of pure form I, for lots 1(b) and 1(d), respectively.

Both kinetics and thermodynamic effects are important during recrystallization. As shown in Fig. 10, the solubility of form II in isopropanol at 70°C (68.3 ± 0.8 mg/ml) is higher than form I (57.7 ± 1.9 mg/ml). Since this solubility difference represents a free energy difference, crystallization of form I is thermodynamically favored as the temperature increases. Slow cooling of hot isopropanol solution was found to reproducibly yield form I, especially in the presence of seed crystals of form I during crystallization (Table 5). Kinetically, though both forms I and II may be present initially, form II would be expected to redissolve and precipitate as form I with slow cooling. The seed crystals help the growth of form I, serving as nuclei for form I during cooling; stirring helps the homogenous distribution of seeds and promotes the conversion of any form II present to form I.

Controlled crystallization conditions involving stirring, slow cooling at the rate of 10°C/15 min with an hour hold at the temperature after each drop, and the addition of seed crystals of form I was implemented in large scale manufacturing of bulk stavudine. Several lots at production scale have been produced. Powder X-ray diffraction of all lots manufactured conformed to form I. Hence a process (Gandhi et al., 1997) was identified and scaled-up which results in reproducible crystallization of polymorphic form I exclusive of forms II and III.

References

Burger, A., Ramberger, R., 1979. On the polymorphism of pharmaceuticals and other molecular crystals I. Mikrochim. Acta 2 (3–4), 259.

Frye, J.S., Maciel, G.E., 1982. Setting the magic angle using a quadrupolar nuclide. J. Magn. Reson. 48, 125.

Gandhi, R.B., Bogardus, J.B., Garofalo, P.M., Marr, T.R., Perrone, R.K., Kaplan, M.A., 1997. D_4T Polymorphic form I Process. U.S. Patent Number: 5, 608, 048.

Grant, D.J.W., Mehdizadeh, M., Chow, A.H.L, Fairbrother, J.E., 1984. Non-linear van't Hoff solubility–temperature plots and their pharmaceutical interpretation. Int. J. Pharm. 18, 25–38.

Gurskaya, G.V., Bochkarev, A.V., Zhdanov, A.S., Dyatkina, N.B., Kraevskii, A.A., 1991. X-ray crystallographic study of 2′,3′-dideoxy-2′,3′-didehydrothymidine conformationally restricted termination substrate of DNA polymerases. Mol. Biol. 25 (2), 483.

Harte, W.E., Starrett, J.E., Martin, J.C., Mansuri, M.M., 1991. Structure studies of the anti-HIV agent 2′,3′-didehydro-2′,3′-dideoxythymidine (d4T). Biochem. Biophys. Res. Comm. 175 (1), 298.

Hendriksen, B.A., 1989. Characterization of calcium fenoprofen 1. Powder dissolution rate and degree of crystallinity. Int. J. Pharm. 60, 243–252.

Hill, J.O., Öjelund, G., Wadsö, I., 1969. Thermochemical results for 'Tris' as a test substance in solution calorimetry. J. Chem. Thermodynamics 1, 111–116.

Hitchcock, M.J.M., 1991. Review: antiviral portrait series, no. 1,2′3′-didehydro-2′3′-dideoxy thymidine (d4T) an anti HIV agent. Antivir. Chem. Chemother. 2, 125–132.

Osborn, B.G., Fearn, T., 1986. Near Infrared Spectroscopy in Food Analysis. Longman Scientific and Technical, Essex, UK, pp. 35–40.

Shefter, E., Higuchi, T., 1963. Dissolution behavior of crystalline solvated and non solvated form of some pharmaceuticals. J. Pharm. Sci. 52, 781–791.

Sutor, D.J., 1958. The structures of the pyrimidines and purines. VI. The crystal structure of theophylline. Acta Cryst. 11, 83.